行政院國家科學委員會專題研究計畫 成果報告

脂溶性大蒜有機硫成分抗粥狀動脈硬化之探討(3/3)
研究成果報告(完整版)

計 畫 類 別 ：個別型
計 畫 編 號 ：NSC 96-2320-B-040-001-
執 行 期 間 ：96 年 08 月 01 日至 97 年 07 月 31 日
執 行 單 位 ：中山醫學大學營養學系

計 畫 主 持 人 ：李宗貴

計畫參與人員： -99：陳暉雯
-99：沈立言
-兼任助理人員：雷燕萍

處 理 方 式 ：本計畫涉及專利或其他智慧財產權，1 年後可公開查詢

中 華 民 國 97 年 11 月 26 日

The Journal of Nutrition
Biochemical, Molecular, and Genetic Mechanisms

Diallyl Disulfide and Diallyl Trisulfide Suppress Oxidized LDL–Induced Vascular Cell Adhesion Molecule and E-Selectin Expression through Protein Kinase A– and B–Dependent Signaling Pathways[1,2]

Yen-Ping Lei,[3] Haw-Wen Chen,[3,4,6] Lee-Yen Sheen,[5] and Chong-Kuei Lii[3,4,6]*

[3]Department of Nutrition, Chung Shan Medical University, Taichung 402, Taiwan; [4]Department of Nutrition, China Medical University, Taichung 404, Taiwan; and [5]Graduate Institute of Food Science and Technology, National Taiwan University, Taipei 106, Taiwan

Abstract

Uptake of oxidized LDL (ox-LDL) by vascular endothelial cells is a critical step in the initiation and development of atherosclerosis. Adhesion molecules are upregulated by ox-LDL and numerous inflammatory cytokines and play a pivotal role in atherogenesis. In this study, we examined whether diallyl sulfide (DAS), diallyl disulfide (DADS), and diallyl trisulfide (DATS), 3 major organosulfur compounds of garlic oil, reduce adhesion molecule expression induced by ox-LDL and, if so, through what mechanism. Human umbilical vein endothelial cells were preincubated with 1 mmol/L DAS, 200 μmol/L DADS, or 100 μmol/L DATS for 16 h and then with 40 mg/L ox-LDL for an additional 24 h. ox-LDL induction of cellular and cell surface expression of E-selectin and vascular cell adhesion molecule (VCAM)-1 was suppressed by garlic allyl sulfides in the order DATS > DADS > DAS. The adhesion of HL-60 cells to endothelial cells was inhibited 27 and 33% and the production of cellular peroxides was inhibited 43 and 50% by DADS and DATS, respectively ($P < 0.05$). ox-LDL alone dephosphorylated protein kinase B (PKB) and cAMP responsive element binding protein (CREB); such deactivation was reversed by DADS and DATS. Electrophoretic mobility shift assay showed that the activation of CREB binding to DNA was consistent with changes in CREB phosphorylation. The protein kinase A (PKA) inhibitor H89 reversed the suppression of VCAM-1 by DADS and DATS, but the phosphoinositide 3-kinase (PI3K) inhibitor wortmannin had no effect. In contrast, wortmannin abolished DADS- and DATS-induced suppression of ox-LDL–induced E-selectin expression. These results suggest that the suppression of ox-LDL–induced E-selectin and VCAM-1 expression by DADS and DATS and, thus, monocyte adhesion to endothelial cells is likely dependent on the PI3K/PKB or PKA/CREB signaling pathway in an adhesion molecule-specific manner. To our knowledge, this is the first report that garlic modulates ox-LDL–mediated leukocyte adhesion to human endothelial cells through the PKB and PKA pathways. J. Nutr. 138: 996–1003, 2008.

Introduction

Cardiovascular disease is one of the leading causes of death among persons living a Western lifestyle, and its etiology is multifactorial (1). Abnormal lipid metabolism, such as increases in LDL concentrations in the circulation and the enhanced oxidation of LDL, is critical for the initiation and development of atherosclerosis (2). Once oxidized LDL (ox-LDL)[7] is taken up by macrophages, it results in the formation of cholesterol-laden foam cells and the fatty streak, the primary histological feature of atherosclerosis (3). ox-LDL also promotes vascular dysfunction by exerting direct cytotoxicity on endothelial cells (4) and enhances the production and release of inflammatory mediators, such as reactive oxygen species

[1] Supported by NSC 94-2320-B-040-034 and NSC 95-2320-B0-040-004 (C.-K. Lii).
[2] Author disclosures: Y.-P. Lei, H.-W. Chen, L.-Y. Sheen, and C.-K. Lii, no conflicts of interest.
[6] These authors contributed equally to this work.
* To whom correspondence should be addressed. E-mail: cklii@csmu.edu.tw.

[7] Abbreviations used: CREB, cAMP responsive element binding protein; DADS, diallyl disulfide; DAS, diallyl sulfide; DATS, diallyl trisulfide; DCF-DA, 2′,7′-dichlorodihydrofluorescein diacetate; EMSA, electrophoretic mobility shift assay; HUVEC, human umbilical vein endothelial cells; ICAM, intercellular adhesion molecule; IL, interleukin; OSC, organosulfur compounds; ox-LDL, oxidized LDL; PI3K, phosphoinositide 3-kinase; PKA, protein kinase A; PKB, protein kinase B; ROS, reactive oxygen species; TNF, tumor necrosis factor; VCAM, vascular cell adhesion molecule.

Manuscript received 11 October 2007. Initial review completed 1 November 2007. Revision accepted 27 February 2008.

(ROS), tumor necrosis factor (TNF)-α, interleukin (IL)-6, arachidonic acid metabolites, and nitric oxide (5). Moreover, through activation of lectine-like ox-LDL receptor-1 (LOX-1) (the receptor that facilitates the uptake of ox-LDL), ox-LDL enhances the expression of P-selectin, vascular cell adhesion molecule (VCAM), intercellular adhesion molecule (ICAM), and monocyte chemotactic protein-1 on cell surfaces, which accelerates the adherence and penetration of leukocytes into the vascular endothelium (6).

Garlic (*Allium sativum* L.) has been used as a flavoring and medicinal agent for hundreds of years. An epidemiological study showed an inverse correlation between garlic consumption and the progression of cardiovascular diseases (7). In addition, numerous in vitro studies demonstrate that garlic can modulate factors associated with cardiovascular diseases, i.e., inhibition of key enzymes involved in cholesterol and lipid synthesis, reduction in platelet aggregation and thrombus formation, enhancement of fibrinolysis, maintenance of vascular tones, and increase in antioxidant defense capability (8). However, in clinical studies conducted during the last 2 decades, the protective effect of garlic on cardiovascular diseases has been inconsistent. The most consistent effect of garlic was to reduce platelet aggregation in 7 of 7 clinical studies in which this was tested (8). However, only 44% (11 of 25) and 60% (6 of 10) of clinical trials reported garlic to be effective in reducing serum cholesterol levels (8,9). The inconsistency among clinical studies could be partly due to the different garlic preparations used (garlic powder, aged garlic extract, or garlic oil), unknown active constituents and their bioavailability, inadequate randomization, different subject health status (normal vs. hypercholesterolemia), gender difference, as well as the duration of different trials (8). Thus more in-depth and appropriately designed studies are warranted.

In addition to its antiatherogenic effect, garlic has diverse biological activities, including antitumorigenesis, antidiabetes, antioxidation, hepatic protection, and immune modulation effects (10,11). Evidence indicates that the health-related functions of garlic largely are due to its rich content of various organosulfur compounds (OSC) (12). Current data suggest that the action of garlic and its OSC in the prevention of atherosclerosis may be related to garlic's modulation of lipid metabolism (13), improvement of vascular endothelial function (14), enhancement of vascular reactivity (15), and modulation of the inflammatory response (16). However, the actual molecular mechanisms that maintain vascular endothelial function have not been fully elucidated.

Protein kinase B (PKB), one of the serine-threonine kinases, is a critical downstream target of phosphoinositide 3-kinase (PI3K). It acts as a key mediator of the PI3K-dependent survival pathway through the phosphorylation and regulation of numerous apoptotic proteins and transcription factors (17,18). When vascular endothelial cells are exposed to ox-LDL, apoptosis increases and endothelial nitric oxide synthase activity and cell migration decrease as the result of PKB dephosphorylation (19,20). The induction of P-selectin and ICAM-1 by ox-LDL in human coronary artery endothelial cells is also negatively related to PKB activation (21). In addition to PI3K/PKB, the cAMP/protein kinase A (PKA) signaling pathway has been shown to play an important role in cilostazol inhibition in TNF-α–induced VCAM-1 and monocyte chemoattractant protein-1 expression in human coronary artery endothelial cells and consequently to suppress monocyte adhesion (22). The inhibition by forskolin of E-selectin and VCAM-1 expression in human umbilical vein endothelial cells (HUVEC) also supports a role of the cAMP/PKA pathway in the modulation of adhesion molecules (23).

Because of the potent action of garlic in vascular function, it is important to determine whether garlic acts by modulating the activation of PKB and PKA. Thus, in this study, we pretreated HUVEC with diallyl sulfide (DAS), diallyl disulfide (DADS), or diallyl trisulfide (DATS), which differ in their number of sulfur atoms, and examined the inhibition of ox-LDL–induced E-selectin and VCAM-1 expression and the resultant changes in PKB and PKA phosphorylation and dephosphorylation.

Materials and Methods

Materials. HUVEC and monocytic HL-60 cells were obtained from Clonetics and Bioresources Collection and Research Center, respectively. DAS and DADS were purchased from Fluka Chemical. DATS was purchased from LKT Laboratories. Medium 199 and RPMI 1640 were from Gibco-BRL. Monoclonal antibodies to E-selectin and VCAM-1 were purchased from Santa Cruz Biotechnology and Chemicon International, respectively. Polyclonal antibodies to PKB, phospho-PKB (Ser473), cAMP responsive element binding protein (CREB), and phospho-CREB (Ser133) were obtained from Cell Signaling Technology. HEPES, heparin, $CuSO_4$, 2′,7′-dichlorodihydrofluorescein diacetate (DCF-DA), wortmannin, and H89 were obtained from Sigma. *bis*-Carboxyethyl-carboxyfluorescein acetoxymethyl ester was ordered from Molecular Probes.

Cell cultures. HUVEC with passages between 7 and 9 were used in this study. Cells were grown in 10 mL of medium 199 supplemented with 20 mmol/L HEPES (pH 7.4), 30 mg/L endothelial cell growth supplement (Upstate Biotechnology), 100 mg/L heparin, 20% fetal bovine serum (Biological Industries), 100,000 U/L penicillin, and 100 mg/L streptomycin at 37°C under 5% CO_2. The HL-60 cells were cultured in T-75 tissue culture flasks in a RPMI 1640 medium supplemented with 10% fetal bovine serum, 100,000 U/L penicillin, and 100 mg/L streptomycin.

LDL isolation and ox-LDL preparation. Blood was collected from healthy volunteers to isolate LDL. Written informed consent as approved by the Review Board for Human Research of the Chung Shan Medical University was signed by all participants. Plasma in the presence of EDTA was used to isolate LDL by sequential ultracentrifugation ($1.019 < d < 1.063$ kg/L) (24). Afterward, native LDL was dialyzed at 4°C for 48 h against 500 volumes of PBS to remove EDTA. To initiate oxidation, LDL (0.5 g protein/L) was exposed to 5 μmol/L $CuSO_4$ for 18 h. The generation of thiobarbituric acid–reactive substances was monitored by the fluorometric method as described by Fraga et al. (25), and the values of malondialdehyde equivalents increased from 0.83 ± 0.17 nmol/mg protein of native LDL to 18.9 ± 1.2 nmol/mg protein of $CuSO_4$–treated LDL. The freshly prepared ox-LDL was dialyzed at 4°C for 48 h against 500 volumes of PBS to remove Cu^{2+} and was sterilized by passage through a 0.45-μm filter. The protein contents of native LDL and the ox-LDL preparations were measured by the Lowry assay (26).

Cell treatments. For each experiment, HUVEC at 80% confluence were incubated with DAS, DADS, or DATS at the indicated concentrations for 16 h and then stimulated with 40 mg/L of ox-LDL for an additional 24 h. Cells were lysed in a phosphorylation lysis buffer (50 mmol/L HEPES, 150 mmol/L NaCl, 200 mmol/L sodium orthovanadate, 10 mmol/L sodium pyrophosphate, 100 mmol/L sodium fluoride, 1 mmol/L EDTA, 1.5 mmol/L magnesium chloride, 10% glycerol, 1% Triton X-100, 1 mmol/L phenylmethylsulphonyl fluoride, and 1 mg/L aprotinin). The cell lysates were then sonicated at 20 W for 15 s. All of the cell extracts were centrifuged at 20,000 × *g* at 4°C for 15 min. The supernatants were recovered and the total protein was analyzed by the Commassie Plus protein assay reagent kit (Pierce Biotechnology). The cytotoxicity of DAS, DADS, and DTAS was determined by MTT 3-(4,5-dimethyl-2-thiazolyl)-2,5-diphenyl-2H-tetrazolium bromide assay (27). Cells treated with different allyl sulfides for 16 h, MTT readings in HUVEC exposed to 1 mmol/L DAS, 200 μmol/L DADS, or 100 μmol/L DATS were 90 ± 3%, 88 ± 4%, or 87 ± 3% ($n = 3$), respectively, of those in control cells.

Immunoblotting. Equal amounts of cellular proteins were electrophoresed in an SDS-polyacrylamide gel, and proteins were then transferred to polyvinylidene difluoride membranes (Amersham Biosciences). Nonspecific binding sites on the membranes were blocked with 5% nonfat milk at 4°C overnight. Membranes were probed with mouse antihuman E-selectin and VCAM-1 or rabbit anti-PKB, phospho-PKB, CREB, phospho-CREB, and β-actin antibody. The membranes were then probed with their respective secondary antibody labeled with horseradish peroxidase. The bands were visualized by using an enhanced chemiluminescence kit (Perkin Elmer Life Science) and quantitated with an AlphaImager 2000 (Alpha Innotech).

RT-PCR for adhesion molecules. Total RNA of HUVEC was extracted by using Trizol reagent (Life Technologies). We used 4 μg total RNA for the synthesis of first-strand cDNA by using Moloney murine leukemia virus RT (Promega) in a 20-μL final volume containing 250 ng oligo-dT and 40 U RNase inhibitor. PCR was carried out in a thermocycler in a 50-μL reaction volume containing 20 μL of cDNA, BioTaq PCR buffer, 50 μmol of each deoxyribonucleotide triphosphate, 1.25 mmol/L $MgCl_2$, and 1 U of BioTaq DNA polymerase (BioLine). Oligonucleotide primers of E-selectin (forward: 5′-TCTCTCAGCT-CTCAC TTTG-3′; reverse: 5′-TTCTTCTTGCTGCAC- CTCT-3′), VCAM-1 (forward: 5′-CCCTTGA CCGGCTGGAGATT-3′; reverse: 5′-CTGGGGGCAACATTGACATAAAGTG-3′), and glyceraldehyde 3-phosphate dehydrogenase (forward: GAGTCAACGGATTTGGTCGT; reverse: TTGATTTTGGAGGGATC TCG) were designed on the basis of published sequences (28). Amplification was performed under standard conditions: denaturation at 94°C for 1 min, 32 cycles of amplification with annealing at 50°C for 1 min, and extension at 72°C for 1 min. The glyceraldehyde 3-phosphate dehydrogenase cDNA level was used as the internal standard. PCR products were resolved in a 1%-agarose gel and were scanned by using a Digital Image Analyzer (Alpha Innotech) and quantitated with an AlphaImager 2000 (Alpha Innotech).

Adhesion molecule expression on cell surfaces. The suppression of garlic allyl sulfides on VCAM-1 and E-selectin expression on plasma membranes was measured by fluorescence flow cytometry. Cells were reacted with fluorescein isothiocyanate–conjugated goat anti-mouse E-selectin or VCAM-1 antibody (Serotec) at 4°C for 45 min in the dark. Cells were washed 3 times with cold PBS and fluorescence was read by use of a Becton Dickinson FACSCalibur (BD Biosciences).

ROS. The production of ROS in HUVEC was measured using a DCF-DA fluorescence flow cytometric assay. At the end of each garlic allyl sulfide and ox-LDL treatment, the fluorogenic substrate solution was added to the M199 medium and incubated for an additional 45 min at 37°C under 5% CO_2. Cells were washed 2 times with cold PBS. The cells were kept cool and then quickly analyzed by Becton Dickinson FACSCalibur.

Monocyte adhesion assay. A total of 1 mL of 1×10^8 HUVEC/L was plated in 24-well plates and allowed to grow to 80% confluence. At the end of garlic allyl sulfide and ox-LDL treatment, a total of 4×10^5 *bis*-carboxyethyl-carboxyfluorescein acetoxymethyl ester–labeled HL-60 cells were added to each well and were coincubated with HUVEC at 37°C for 30 min. The wells were washed and filled with cell culture medium, and the plates were sealed, inverted, and centrifuged at $100 \times g$ for 5 min to remove nonadherent HL-60 cells. Bound HL-60 cells were lysed in a 1% SDS solution and the fluorescence intensity was determined in a PerkinElmer HTS 7000 plate reader (PerkinElmer Instruments) with an excitation wavelength of 490 nm and an emission wavelength of 520 nm. The control study showed that fluorescence is a linear function of HL-60 in the range of 3,000 to 60,000 cells/well. Based on the standard curve obtained, the results are reported as the number of HL-60 adherent cells per well (29).

Electrophoretic mobility shift assay (EMSA). Nuclear extraction and EMSA were performed according to our previous study (30). The LightShift Chemiluminescent EMSA kit from Pierce Chemical and synthetic biotin-labeled double-stranded CREB consensus oligonucleotides (5′-AGAGATTGCCTGACGTCAGAGAGCTAG-3′) were used to measure the effect of DADS or DATS on CREB nuclear protein–DNA binding activity. Nuclear extract (2 μg), poly(dI-dC), and biotin-labeled double-stranded CREB oligonucleotides were mixed with the binding buffer (to a final volume of 20 μL) and were incubated at room temperature for 30 min. The nuclear protein–DNA complex was separated by electrophoresis on a 6% Tris-boric acid-EDTA-polyacrylamide gel and was then electrotransferred to a Hybond-N^+ membrane (Amersham Pharmacia Biotech). Next, the membrane was treated with streptavidin-horseradish peroxidase, and the nuclear protein–DNA bands were developed by using an enhanced chemiluminescence kit.

Statistical analysis. Values are expressed as means ± SD, $n = 3$. Statistical analysis was performed with commercially available software (SAS Institute). Data were analyzed by means of 1-way ANOVA, and the significant difference among treatment means was assessed by Tukey's test. Differences of $P < 0.05$ were considered significant.

Results

Dose and time responses of allyl sulfides on E-selectin expression. We first determined the optimal concentration of ox-LDL for the induction of E-selectin. In the presence of 20–200 mg/L of ox-LDL, E-selectin expression was induced at concentrations >40 mg/L ($P < 0.05$) (**Fig. 1***A*). After pretreatment with various concentrations of DADS (100–400 μmol/L) or DATS (50–200 μmol/L), the induction of E-selectin by ox-LDL was suppressed ($P < 0.05$), and maximal inhibition occurred at 100 μmol/L of DATS (Fig. 1*B*). The time course of the effects of 200 μmol/L DADS and 100 μmol/L DATS on E-selectin expression was also examined. Significant suppression by DADS and DATS started at 16 and 8 h, respectively (Fig. 1*C*). On the basis of these findings, the concentrations of DADS and DATS tested in the following experiments were 200 and 100 μmol/L, respectively, with a pretreatment period of 16 h and an ox-LDL concentration of 40 mg/L.

Next, we determined the potency of DADS, DATS, and DAS in suppressing ox-LDL induction of adhesion molecule protein and mRNA. Immunoblots indicated that DADS and DATS were effective not only in suppressing E-selectin but also in suppressing the expression of VCAM-1 (**Fig. 2***A*). By contrast, DAS even at a dose of 1 mmol/L had a slight effect ($P > 0.05$) on both E-selectin and VCAM-1 protein levels. RT-PCR showed that the suppression by the 3 garlic allyl sulfides of E-selectin and VCAM-1 mRNA was similar to that noted for the proteins (Fig. 2*B*). DATS resulted in the greatest reduction in E-selectin and VCAM-1 mRNA, followed by DADS. Again, DAS had the least effect.

Adhesion of HL-60 to HUVEC. The expression of both E-selectin and VCAM-1 on the cell surface of HUVEC was first determined by flow cytometry. In the presence of ox-LDL, the amounts of E-selectin (**Table 1**) on the cell surface of HUVEC was increased by 3-fold ($P < 0.05$). This increase was suppressed by each of the allyl sulfides ($P < 0.05$). The inhibitory potency of the 3 garlic components was in the order DATS > DADS > DAS. Similar to E-selectin, the structure-function relationship among the 3 garlic allyl sulfides was also noted for the suppression of VCAM-1 expression (Table 1).

Consistent with the increase in adhesion molecule expression on HUVEC, ox-LDL markedly increased the adherence of HL-60 on endothelial cells as compared with control cells ($P < 0.05$) (Table 1). Pretreatment of cells with DAS, DADS, or DATS suppressed this increase in adherence of HL-60 cells by 14, 27, and 33%, respectively ($P < 0.05$). Again, the extent of the

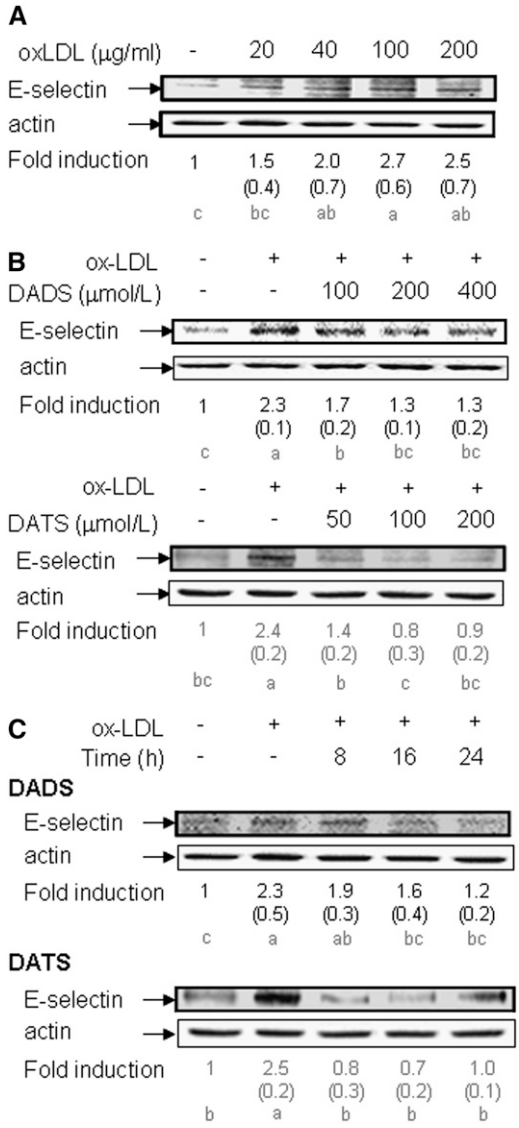

FIGURE 1 Time- and dose-dependent changes in E-selectin expression levels in HUVEC caused by DADS or DATS in the absence or presence of ox-LDL. Cells at 80% confluence were treated with 0–200 mg/L ox-LDL for 24 h, and changes in E-selectin levels were determined by immunoblot assay (*A*). Cells were pretreated with various concentrations of DADS or DATS for 16 h (*B*) or with 200 μmol/L DADS or 100 μmol/L DATS for different times (*C*) followed by stimulation with 40 mg/L ox-LDL for an additional 24 h. The protein was quantified by densitometry, and the level in control cells was set 1. Values are means (SD), $n = 3$. Means without a common letter differ, $P < 0.05$.

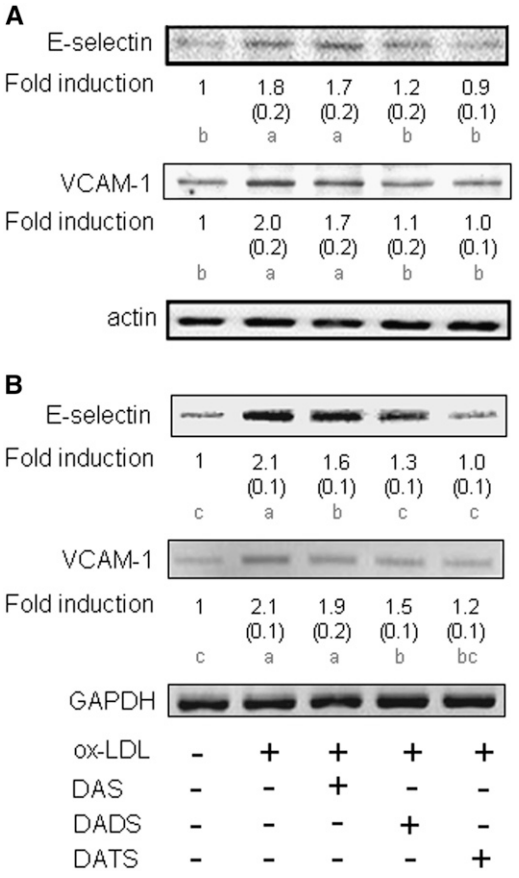

FIGURE 2 Garlic allyl sulfides suppress ox-LDL–induced E-selectin and VCAM-1 protein (*A*) and mRNA (*B*) expression. HUVEC were pretreated with 1 mmol/L DAS, 200 μmol/L DADS, or 100 μmol/L DATS for 16 h and were then incubated with 40 mg/L ox-LDL for an additional 24 h. Protein and mRNA levels were determined by immunoblot assay and RT-PCR, as described in Materials and Methods. The protein was quantified by densitometry, and the level in control cells was set 1. Values are means (SD), $n = 3$. Means without a common letter differ, $P < 0.05$.

reduction was related to the number of sulfur atoms of the 3 garlic allyl sulfides.

Intracellular ROS production. Changes in intracellular ROS production were determined by DCF-DA assay. With ox-LDL alone, cellular fluorescence intensity in HUVEC was 4-fold that of control cells ($P < 0.05$) (Table 1). After pretreatment with DADS or DATS, ox-LDL–induced oxidative stress was significantly suppressed, and cellular ROS levels were 56 and 49%, respectively, of that with ox-LDL alone ($P < 0.05$). DAS, however, had only a minor effect on ROS production.

PKB and CREB activation. To determine whether DADS and DATS ameliorate adhesion molecule expression by modulating the phosphorylation or dephosphorylation states of PKB and CREB, we performed an immunoblot assay (**Fig. 3**). As noted, ox-LDL resulted in PKB dephosphorylation in HUVEC. After pretreatment with DADS or DATS, the deactivation of PKB by ox-LDL was prevented ($P < 0.05$). Also, the prevention of PKB dephosphorylation by DADS and DATS paralleled their

TABLE 1 Suppression by DAS, DADS, and DATS of ox-LDL–induced adhesion molecule expression on cell surfaces, adhesion of HL-60 cells to endothelial cells, and production of ROS[1,2]

	E-selectin	VCAM-1	HL-60 cells	ROS
	Fluorescence		$n \times 10^3$	Fluorescence
Control	3.9 ± 0.1[e]	3.7 ± 0.4[d]	13.4 ± 1.2[d]	3.7 ± 0.4[c]
ox-LDL	16.6 ± 0.4[a]	15.5 ± 0.2[a]	40.8 ± 4.0[a]	14.6 ± 0.9[a]
DAS + ox-LDL	11.4 ± 1.0[b]	13.1 ± 0.0[b]	35.2 ± 1.4[b]	12.8 ± 2.3[a]
DADS + ox-LDL	9.1 ± 0.7[c]	12.5 ± 0.4[b]	29.8 ± 1.6[c]	8.3 ± 1.0[b]
DATS + ox-LDL	7.3 ± 1.3[d]	10.3 ± 0.9[c]	27.4 ± 0.9[c]	7.3 ± 1.3[b]

[1] Values are means ± SD, $n = 3$.
[2] Means in a column without a common letter differ, $P < 0.05$.

suppression of both E-selectin and VCAM-1 expression. In the presence of wortmannin, a PI3K inhibitor, the effect of DADS and DATS on restoring PKB activation was blocked and the suppression by the 2 allyl sulfides of E-selectin expression was diminished ($P < 0.05$). In contrast to E-selectin, wortmannin did not reverse the suppression of VCAM-1 expression induced by DADS and DATS.

In addition to the deactivation of PKB, CREB was also dephosphorylated in the presence of ox-LDL (Fig. 3). After pretreatment with DADS or DATS, the level of phospho-CREB was normalized to the level in control cells and differed from that in cells treated with ox-LDL alone ($P < 0.05$). When the PKA inhibitor H89 was included, the level of phosphorylated CREB was not normalized. In agreement with this finding, the suppression by DADS and DATS of VCAM-1 was abolished by H89 ($P < 0.05$), and the level of VCAM-1 returned to that in cells incubated with ox-LDL alone. H89 partially reversed the suppression of E-selectin by DADS and DATS.

DNA binding activity of CREB. Consistent with our findings for changes in CREB phosphorylation, EMSA showed that, upon treatment with ox-LDL alone, the DNA binding activity of CREB nuclear protein was markedly lower (**Fig. 4**, lane 2) than that of the control (lane 1). DADS and DATS prevented the deactivation of CREB by ox-LDL (lanes 3 and 4). The prevention of CREB binding to DNA by allyl sulfides was diminished in the presence of H89 (lanes 7 and 8) but not wortmannin (lanes 5 and 6).

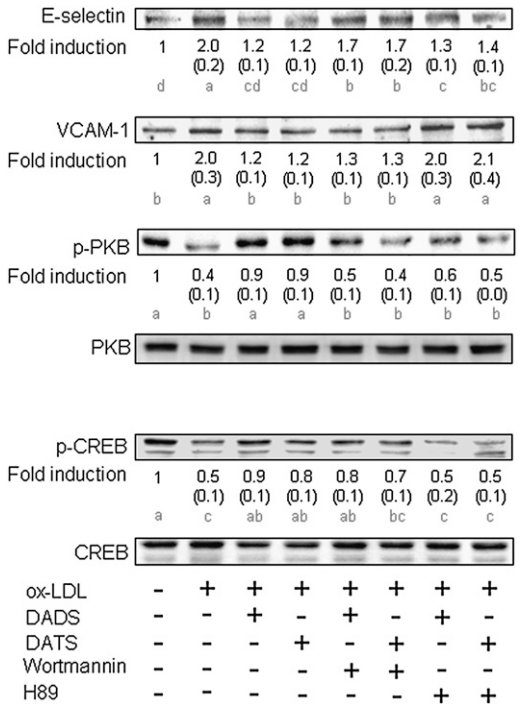

FIGURE 3 Changes in PKB and CREB phosphorylation in cultured HUVEC caused by DADS and DATS. Cells were incubated with either 200 μmol/L DADS or 100 μmol/L DATS for 16 h and were then treated with 40 mg/L ox-LDL for an additional 24 h. For inhibitor treatments, wortmannin (100 nmol/L) or H89 (5 μmol/L) was added 1 h before the addition of DADS or DATS. The protein was quantified by densitometry, and the level in control cells was set 1. Values are means (SD), $n = 3$. Means without a common letter differ, $P < 0.05$.

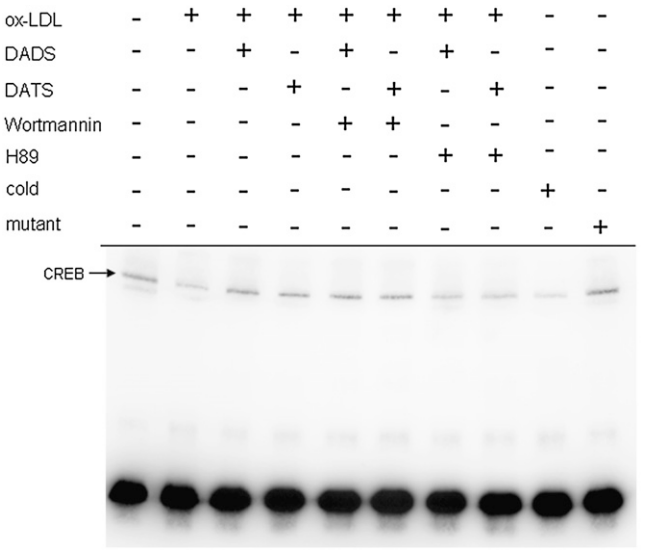

FIGURE 4 The DNA binding activity of nuclear CREB protein. HUVEC were preincubated with 200 μmol/L DADS or 100 μmol/L DATS for 16 h and were then stimulated by 40 mg/L ox-LDL for an additional 24 h. Wortmannin (100 nmol/L) or H89 (5 μmol/L) was added 1 h before allyl sulfide treatment. Nuclear extracts were used to measure the CREB nuclear protein DNA binding activity by EMSA. An unlabeled double-stranded CREB oligonucleotide (50 ng) was added for the competition assay, and an unlabeled double-stranded mutant CREB oligonucleotide (50 ng) was added for the specificity assay. Data shown are representative of 3 independent experiments.

Discussion

Although, the protection provided by garlic in clinical trials remains controversial, epidemiological and in vitro studies suggest that garlic can reduce the progression of cardiovascular disease as a result of its hypolipidemic, antithrombosis, and antioxidative effects (7–9). In this study, we further showed that DADS and DATS, 2 major OSC of garlic oil, effectively suppress the ox-LDL induction of HL-60 cell adhesion to HUVEC, and that this could be attributed to their downregulation of ICAM-1 and VCAM-1 mRNA and protein expression. Moreover, this effect on ox-LDL–induced E-selectin and VCAM-1 expression is likely to occur via the PI3K/PKB and PKA/CREB signaling pathways. These findings provide insight into the molecular action of DADS and DATS in protecting blood vessels against ox-LDL–triggered atherosclerosis.

Increases in adhesion molecule expression and adhesion of leukocytes to the vascular endothelial cell surface occur at an early stage of atherosclerosis (31). Interruption of the abnormal induction of adhesion molecules under certain circumstances, such as chronic inflammation, is thought to be effective for ameliorating this blood vessel disease (32). Proinflammatory cytokines, including TNF-α and IL-1, are effective inducers of adhesion molecules, and the NF-κB–dependent pathway has been reported to play an important role in this induction (33). Therefore, most recent studies that have investigated the action of health foods and their active phytochemicals against the abnormal induction of adhesion molecules have examined the role of NF-κB. For instance, garlic's suppression of the induction of ICAM-1 and VCAM-1 by IL-1-α in human coronary artery endothelial cells was attributed to its inhibition of NF-κB activation (34,35). In fact, adhesion molecules are also highly inducible by numerous stimuli related to mitogen-activated

protein kinases, PKA, and PI3K/PKB signaling (36–39). In human coronary artery endothelial cells, ox-LDL induction of ICAM-1 and P-selectin expression was shown to be associated with the dephosphorylation of PKB (21). On the basis of *1*) the parallel responses of DADS and DATS in the suppression of ox-LDL–induced E-selectin expression and changes in PKB phosphorylation and *2*) the reversal of the suppression of E-selectin by wortmannin, the evidence from this study suggests that the PKB signaling pathway is likely to play an important role in the suppression by DADS and DATS of E-selectin induced by ox-LDL.

By contrast, the inability of wortmannin to reverse the suppression of VCAM-1 induction by ox-LDL suggests that the mechanism by which garlic allyl sulfides inhibit VCAM-1 is different from that for E-selectin. The modulation of E-selectin, VCAM-1, and ICAM-1 transcription may share common regulatory signals; however, the existence of gene-specific signal mechanisms cannot be excluded (40). Pober et al. (41) indicated that the elevation of cyclic AMP selectively inhibited endothelial cell expression of TNF-induced E-selectin and VCAM-1, but not of ICAM-1. In this study, the suppression by DADS and DATS of ox-LDL–induced VCAM-1 expression was fully reversed by the PKA inhibitor H89, but only a partial reversion was noted for E-selectin expression. The results of the H89 and wortmannin studies strongly indicate that the suppression by garlic allyl sulfides of E-selectin induction by ox-LDL is primarily related to the PI3K/PKB signaling pathway. By contrast, the PKA/CREB pathway, rather than PI3K/PKB signaling, plays the key role in the action of DADS and DATS against VCAM-1 induction. To our knowledge, this is the first report that garlic modulates ox-LDL–mediated leukocyte adhesion to human endothelial cells through the PKB and PKA pathways. Further study is required to clearly distinguish the actual role of PKB and PKA in the DADS- and DATS-induced suppression of E-selectin and VCAM-1 transcription.

Adhesion molecules, including VCAM-1 and E-selectin, are critical in the interactions between monocytes and the endothelium, and the recruitment of circulating monocytes to vascular endothelial cells is an early step in the development of atherosclerosis (31). Interruption of adhesion molecule overexpression on the cell membrane was thought to prevent the progress of atherosclerosis. In this study, DADS and DATS not only effectively suppressed cellular E-selectin and VCAM-1 mRNA and protein levels but also decreased their expression on the cell surface of HUVEC. DADS and DATS thus result in inhibition of monocyte adhesion to endothelial cells. This evidence explains, at least in part, the antiatherogenic action of DADS and DATS against ox-LDL–induced blood vessel damage. Decreases in E-selectin and VCAM-1 expression on the cell membrane could be the result of downregulation of gene transcription. However, it is also possible that it is the result of interference with the transportation of adhesion molecules from the cytosol to the cell surface (42). At present, it is not clear whether DADS and DATS interrupt E-selectin and VCAM-1 transportation and what roles PKA- and PKB-dependent signaling play in the modulation of adhesion molecule transportation. All these processes remain to be studied.

Oxidative stress is a key inducer of ICAM, VCAM, and E-selectin expression by ox-LDL and proinflammatory cytokines (43). This explains why antioxidants, e.g., *N*-acetylcysteine and α-tocopherol, may inhibit IL-β– and ox-LDL–induced VCAM-1 and ICAM-1 expression in endothelial cells with a subsequent decrease in leukocyte adhesion (44,45). Garlic and its OSC have been shown to have antioxidant properties in in vivo and in vitro studies (30,46–48). In this study, the effectiveness of garlic allyl sulfides in decreasing cellular ROS production induced by ox-LDL supports their potent antioxidant properties. Furthermore, the good correlation ($r = 0.87$, $P < 0.0001$) between the inhibition of cellular ROS production and the suppression of adhesion molecule expression of the 3 garlic allyl sulfides tested suggests that the protection against ox-LDL–induced E-selectin and VCAM-1 overexpression by DADS and DATS is partly due to their antioxidant activity. However, in cancer cells, such as LNCaP cells, an increase in ROS production by DATS has been reported (49). This indicates that not all cells respond identically to garlic OSC in the production of ROS and possibly in the modulation of a number of redox-dependent signaling pathways and associated protein expression.

Structure-function relationship studies often are conducted to determine the relative biological activities of phytochemicals with common structures, including green tea polyphenols and soy isoflavones (50,51). In addition, it has been shown that both the number of sulfur atoms and the number of allyl groups in a garlic sulfur-containing molecule are important determinants of organ specificity and chemopreventive efficacy (52). The structure-activity relationship studies have shown that DADS and DATS have comparable activity against Benzo(a)pyrene-induced forestomach tumorigenesis in mice, and both compounds are more effective than DAS (53,54). Recently, we reported that the efficacy of DAS, DADS, and DATS in upregulating the transcription of the π form of glutathione S-transferase, a phase II drug-metabolizing enzyme, was positively correlated with the number of sulfur atoms (55,56). In this study, we further showed that there is a similar structure-activity relationship among DAS, DADS, and DATS in the suppression of E-selectin and VCAM-1 overexpression and monocyte adhesion to vascular endothelial cells induced by ox-LDL.

It is important to determine whether the effective concentration of garlic allyl sulfides to suppress adhesion molecule expression found in this study is achievable via the dietary supplement of garlic oil. Given that DATS accounts for 35% of garlic oil (56) and the high absorption of garlic OSC (57), we estimate that dietary garlic oil supplementation at 2.0 mg/kg body weight could result in a circulating DATS concentration of 50 μmol/L. This means that a 70-kg man requires 140 mg garlic oil/d, corresponding to 56 g raw garlic cloves (1 kg raw garlic yields 2.5 g garlic oil by steam distillation). In a clinical study, Bordia (58) showed that a 0.25 mg/kg body weight garlic oil supplement for 10 mo reduced circulating cholesterol and triglycerides in patients with coronary heart disease.

In summary, DADS and DATS, the 2 major OSC of garlic oil, effectively suppress ox-LDL–induced E-selectin and VCAM-1 expression and, thus, decrease monocyte adhesion to endothelial cells. The suppression of E-selectin overexpression by DADS and DATS is likely via the PI3K/PKB signaling pathway; however, PKA/CREB signaling seems to be the key pathway in the suppression of VCAM-1 expression. These findings may provide insight into the mechanisms of garlic's protection against atherosclerosis.

Literature Cited

1. Beilin LJ. Lifestyle and hypertension–an overview. Clin Exp Hypertens. 1999;21:749–62.
2. Kita T, Kume N, Minami M, Hayashida K, Murayama T, Sano H, Moriwaki H, Kataoka H, Nishi E, et al. Role of oxidized LDL in atherosclerosis. Ann N Y Acad Sci. 2001;947:199–206.

3. Babaev VR, Patel MB, Semenkovich CF, Fazio S, Linton MF. Macrophage lipoprotein lipase promotes foam cell formation and atherosclerosis in low density lipoprotein receptor-deficient mice. J Biol Chem. 2000;275: 26293–9.
4. Morawietz H, Duerrschmidt N, Niemann B, Galle J, Sawamura T, Holtz J. Induction of the oxLDL receptor LOX-1 by endothelin-1 in human endothelial cells. Biochem Biophys Res Commun. 2001;284: 961–5.
5. Zmijewski JW, Moellering DR, Le Goffe C, Landar A, Ramachandran A, Darley-Usmar VM. Oxidized LDL induces mitochondrially associated reactive oxygen/nitrogen species formation in endothelial cells. Am J Physiol Heart Circ Physiol. 2005;289:H852–61.
6. Kita T. LOX-1, a possible clue to the missing link between hypertension and atherogenesis. Circ Res. 1999;84:1113–5.
7. Kendler BS. Garlic (*Allium sativum*) and onion (*Allium cepa*): a review of their relationship to cardiovascular disease. Prev Med. 1987;16: 670–85.
8. Rahman K, Lowe GM. Garlic and cardiovascular disease: a critical review. J Nutr. 2006;136:736S–40S.
9. Alder R, Lookinland S, Berry JA, Williams M. A systematic review of the effectiveness of garlic as an antihyperlipidemic agent. J Am Acad Nurse Pract. 2003;15:120–9.
10. Agarwal KC. Therapeutic actions of garlic components. Med Res Rev. 1996;16:111–24.
11. Rivlin RS. Historical perspective on the use of garlic. J Nutr. 2001;131: 951S–4S.
12. Amagase H. Clarifying the real bioactive constituents of garlic. J Nutr. 2006;136:716S–25S.
13. Adler AJ, Holub BJ. Effect of garlic and fish-oil supplementation on serum lipid and lipoprotein concentrations in hypercholesterolemic men. Am J Clin Nutr. 1997;65:445–50.
14. Williams MJ, Sutherland WH, McCormick MP, Yeoman DJ, de Jong SA. Aged garlic extract improves endothelial function in men with coronary artery disease. Phytother Res. 2005;19:314–9.
15. Ganado P, Sanz M, Padilla E, Tejerina T. An in vitro study of different extracts and fractions of *Allium sativum* (garlic): vascular reactivity. J Pharmacol Sci. 2004;94:434–42.
16. Sela U, Ganor S, Hech I, Brill A, Miron T, Rabinkov A, Wilchek M, Mirelman D, Lider O, Hershkoviz R. Allicin inhibits SDF-1alpha-induced T cell interactions with fibronectin and endothelial cells by down-regulating cytoskeleton rearrangement, Pyk-2 phosphorylation and VLA-4 expression. Immunology. 2004;111:391–9.
17. Downward J. Mechanisms and consequences of activation of protein kinase B/Akt. Curr Opin Cell Biol. 1998;10:262–7.
18. Sun RQ, Tu YJ, Yan JY, Willis WD. Activation of protein kinase B/Akt signaling pathway contributes to mechanical hypersensitivity induced by capsaicin. Pain. 2006;120:86–96.
19. Du XL, Edelstein D, Dimmeler S, Ju Q, Sui C, Brownlee M. Hyperglycemia inhibits endothelial nitric oxide synthase activity by posttranslational modification at the Akt site. J Clin Invest. 2001;108: 1341–8.
20. Chavakis E, Dernbach E, Hermann C, Mondorf UF, Zeiher AM, Dimmeler S. Oxidized LDL inhibits vascular endothelial growth factor-induced endothelial cell migration by an inhibitory effect on the Akt/endothelial nitric oxide synthase pathway. Circulation. 2001;103: 2102–7.
21. Chen H, Li D, Chen J, Roberts GJ, Saldeen T, Mehta JL. EPA and DHA attenuate ox-LDL-induced expression of adhesion molecules in human coronary artery endothelial cells via protein kinase B pathway. J Mol Cell Cardiol. 2003;35:769–75.
22. Park SY, Lee JH, Kim CD, Lee WS, Park WS, Han J, Kwak YG, Kim KY, Hong KW. Cilostazol suppresses superoxide production and expression of adhesion molecules in human endothelial cells via mediation of cAMP-dependent protein kinase-mediated maxi-K channel activation. J Pharmacol Exp Ther. 2006;317:1238–45.
23. Ghersa P, Hooft van Huijsduijnen R, Whelan J, Cambet Y, Pescini R, DeLamarter JF. Inhibition of E-selectin gene transcription through a cAMP-dependent protein kinase pathway. J Biol Chem. 1994;269: 29129–37.
24. Claise C, Edeas M, Chaouchi N, Chalas J, Capel L, Kalimouttou S, Vazquez A, Lindenbaum A. Oxidized-LDL induce apoptosis in HUVEC but not in the endothelial cell line EA.hy 926. Atherosclerosis. 1999;147:95–104.
25. Fraga CG, Leibovitz BE, Tappel AL. Lipid peroxidation measured as thiobarbituric acid-reactive substances in tissue slices: characterization and comparison with homogenates and microsomes. Free Radic Biol Med. 1988;4:155–61.
26. Lowry OH, Rosebrough NJ, Farr AL, Randall RJ. Protein measurement with the Folin phenol reagent. J Biol Chem. 1951;193:265–75.
27. Denizot F, Lang R. Rapid colorimetric assay for cell growth and survival. Modifications to the tetrazolium dye procedure giving improved sensitivity and reliability. J Immunol Methods. 1986;89: 271–7.
28. Meagher L, Mahiouz D, Sugars K, Burrows N, Norris P, Yarwood H, Becker-Andre M, Haskard DO. Measurement of mRNA for E-selectin, VCAM-1 and ICAM-1 by reverse transcription and the polymerase chain reaction. J Immunol Methods. 1994;175:237–46.
29. Yoshida M, Chien LJ, Yasukochi Y, Numano F. Differentiation-induced transmigration of HL60 cells across activated HUVEC monolayer involves E-selectin-dependent mechanism. Ann N Y Acad Sci. 2000; 902:307–10.
30. Tsai CW, Chen HW, Yang JJ, Sheen LY, Lii CK. Diallyl disulfide and diallyl trisulfide up-regulate the expression of the pi class of glutathione S-transferase via an AP-1-dependent pathway. J Agric Food Chem. 2007;55:1019–26.
31. O'Brien KD, McDonald TO, Chait A, Allen MD, Alpers CE. Neovascular expression of E-selectin, intercellular adhesion molecule-1, and vascular cell adhesion molecule-1 in human atherosclerosis and their relation to intimal leukocyte content. Circulation. 1996;93: 672–82.
32. Stangl V, Lorenz M, Ludwig A, Grimbo N, Guether C, Sanad W, Ziemer S, Martus P, Baumann G, Stangl K. The flavonoid phloretin suppresses stimulated expression of endothelial adhesion molecules and reduces activation of human platelets. J Nutr. 2005;135:172–8.
33. Dhawan S, Singh S, Aggarwal BB. Induction of endothelial cell surface adhesion molecules by tumor necrosis factor is blocked by protein tyrosine phosphatase inhibitors: role of the nuclear transcription factor NF-kappa B. Eur J Immunol. 1997;27:2172–9.
34. Rassoul F, Salvetter J, Reissig D, Schneider W, Thiery J, Richter V. The influence of garlic (Allium sativum) extract on interleukin 1alpha-induced expression of endothelial intercellular adhesion molecule-1 and vascular cell adhesion molecule-1. Phytomedicine. 2006;13:230–5.
35. Ide N, Lau BH. Garlic compounds minimize intracellular oxidative stress and inhibit nuclear factor-kappa b activation. J Nutr. 2001;131: 1020S–6S.
36. Hu Y, Kiely JM, Szent BE, Rosenzweig A, Gimbrone MA Jr. E-selectin-dependent signaling via the mitogen-activated protein kinase pathway in vascular endothelial cells. J Immunol. 2000;165:2142–8.
37. Kim I, Moon SO, Kim SH, Kim HJ, Koh YS, Koh GY. Vascular endothelial growth factor expression of intercellular adhesion molecule 1 (ICAM-1), vascular cell adhesion molecule 1 (VCAM-1), and E-selectin through nuclear factor-kappa B activation in endothelial cells. J Biol Chem. 2001;276:7614–20.
38. Ollivier V, Parry GC, Cobb RR, de Prost D, Mackman N. Elevated cyclic AMP inhibits NF-kappaB-mediated transcription in human monocytic cells and endothelial cells. J Biol Chem. 1996;271:20828–35.
39. Schmidt A, Geigenmuller S, Volker W, Buddecke E. The antiatherogenic and antiinflammatory effect of HDL-associated lysosphingolipids operates via Akt →NF-kappaB signalling pathways in human vascular endothelial cells. Basic Res Cardiol. 2006;101:109–16.
40. Cominacini L, Garbin U, Pasini AF, Davoli A, Campagnola M, Contessi GB, Pastorino AM, Lo Cascio V. Antioxidants inhibit the expression of intercellular cell adhesion molecule-1 and vascular cell adhesion molecule-1 induced by oxidized LDL on human umbilical vein endothelial cells. Free Radic Biol Med. 1997;22:117–27.
41. Pober JS, Slowik MR, De Luca LG, Ritchie AJ. Elevated cyclic AMP inhibits endothelial cell synthesis and expression of TNF-induced endothelial leukocyte adhesion molecule-1, and vascular cell adhesion molecule-1, but not intercellular adhesion molecule-1. J Immunol. 1993;150:5114–23.
42. Frenette PS, Wagner DD. Adhesion molecules–Part 1. N Engl J Med. 1996;334:1526–9.
43. Kobayashi N, Mita S, Yoshida K, Honda T, Kobayashi T, Hara K, Nakano S, Tsubokou Y, Matsuoka H. Celiprolol activates eNOS through the PI3K-Akt pathway and inhibits VCAM-1 Via NF-kappaB induced by oxidative stress. Hypertension. 2003;42:1004–13.

44. Faruqi RM, Poptic EJ, Faruqi TR, De La Motte C, DiCorleto PE. Distinct mechanisms for N-acetylcysteine inhibition of cytokine-induced E-selectin and VCAM-1 expression. Am J Physiol. 1997;273: H817–26.
45. Martin A, Foxall T, Blumberg JB, Meydani M. Vitamin E inhibits low-density lipoprotein-induced adhesion of monocytes to human aortic endothelial cells in vitro. Arterioscler Thromb Vasc Biol. 1997;17:429–36.
46. Borek C. Antioxidant health effects of aged garlic extract. J Nutr. 2001; 131:1010S–5S.
47. Lau BH. Suppression of LDL oxidation by garlic. J Nutr. 2001;131: 985S–8S.
48. Hsu CC, Yen HF, Yin MC, Tsai CM, Hsieh CH. Five cysteine-containing compounds delay diabetic deterioration in Balb/cA mice. J Nutr. 2004;134:3245–9.
49. Kim YA, Xiao D, Xiao H, Powolny AA, Lew KL, Reilly ML, Zeng Y, Wang Z, Singh SV. Mitochondria-mediated apoptosis by diallyl trisulfide in human prostate cancer cells is associated with generation of reactive oxygen species and regulated by Bax/Bak. Mol Cancer Ther. 2007;6:1599–609.
50. Wan SB, Chen D, Dou QP, Chan TH. Study of the green tea polyphenols catechin-3-gallate (CG) and epicatechin-3-gallate (ECG) as proteasome inhibitors. Bioorg Med Chem. 2004;12:3521–7.
51. Chun HS, Chang HJ, Choi EH, Kim HJ, Ku KH. Molecular and absorption properties of 12 soy isoflavones and their structure-activity relationship with selected biological activities. Biotechnol Lett. 2005;27: 1105–11.
52. Singh SV, Pan SS, Srivastava SK, Xia H, Hu X, Zaren HA, Orchard JL. Differential induction of NAD(P)H:quinone oxidoreductase by anti-carcinogenic organosulfides from garlic. Biochem Biophys Res Commun. 1998;244:917–20.
53. Sparnins VL, Barany G, Wattenberg LW. Effects of organosulfur compounds from garlic and onions on benzo[a]pyrene-induced neoplasia and glutathione S-transferase activity in the mouse. Carcinogenesis. 1988;9:131–4.
54. Hu X, Benson PJ, Srivastava SK, Xia H, Bleicher RJ, Zaren HA, Awasthi S, Awasthi YC, Singh SV. Induction of glutathione S-transferase pi as a bioassay for the evaluation of potency of inhibitors of benzo(a)pyrene-induced cancer in a murine model. Int J Cancer. 1997; 73:897–902.
55. Tsai CW, Yang JJ, Chen HW, Sheen LY, Lii CK. Garlic organosulfur compounds upregulate the expression of the pi class of glutathione S-transferase in rat primary hepatocytes. J Nutr. 2005;135:2560–5.
56. Wu CC, Sheen LY, Chen HW, Kuo WW, Tsai SJ, Lii CK. Differential effects of garlic oil and its three major organosulfur components on the hepatic detoxification system in rats. J Agric Food Chem. 2002;50: 378–83.
57. Nagae S, Ushijima M, Hatono S, Imai J, Kasuga S, Matsuura H, Itakura Y, Higashi Y. Pharmacokinetics of the garlic compound S-allylcysteine. Planta Med. 1994;60:214–7.
58. Bordia A. Effect of garlic on blood lipids in patients with coronary heart disease. Am J Clin Nutr. 1981;34:2100–3.

Diallyl Disulfide and Diallyl Trisulfide Protect Endothelial Cells Against Oxidized Low-density Lipoprotein Down-Regulation of eNOS Expression and Activation

Introduction

Atherosclerosis is a severe disease worldwide, which leads to alterations and lesions in the inner walls of the blood vessels (Ross, 1993). Although its etiology is known to be multifactorial, endothelial dysfunctions, especially elicited by oxidized low-density lipoprotein (ox-LDL), play a critical role in the pathogenesis of atherosclerosis (Steinberg, 1997; Witztum and Steinberg, 1991). ox-LDL is taken up by macrophages, it results in the formation of cholesterol-laden foam cells and the fatty streak, the primary histological feature of atherosclerosis (Babaev et al., 2000). ox-LDL also promotes vascular dysfunction by exerting direct cytotoxicity on endothelial cells (Morawietz et al., 2001) and enhances the production and release of inflammatory mediators, such as reactive oxygen species, TNFα, IL-6, and arachidonic acid metabolites (Zmijewski et al., 2005). Moreover, ox-LDL inhibits NO production and thus, NO-mediated responses in endothelial cells (Blair et al., 1999; Ji et al., 2006; Xu et al., 2004). Dysregulation of NO production has been demonstrated to play a role in the pathogenesis of several cardiovascular disorders including essential hypertension, reperfusion injury, atherosclerosis, and the myocardial depression associated with (septic) shock (Loscalzo and Welch, 1995). Thus, NO status in endothelium is critical in maintaining the normal functions of blood vessels (Kawashima, 2004; Lloyd-Jones and Bloch, 1996; Moncada and Higgs, 2006).

Endothelial nitric-oxide synthase (eNOS) is a peripheral membrane protein in endothelial cells because of its co-translational *N*-myristoylation and post-translational cysteine palmitoylation (Liu et al., 1995). Membrane associated eNOS is localized in caveolae (Feron et al., 1998; Michel et al., 1997) and directly bound to caveolin-1 (Michel et al., 1997). eNOS plays an important role in cardiovascular homeostasis including not only regulation of vascular tone but also platelet aggregation, smooth muscular proliferation, and leukocyte adhesion to endothelial cells (Alderton et al., 2001; Bredt, 1999; Loscalzo and Welch, 1995). It is well documented that eNOS activity is highly regulated by post-translational modifications, such as Akt-induced phosphorylation (Fulton et al., 1999; Garcia-Cardena et al., 1998) and its interaction with several regulatory proteins such as heat shock protein 90 (HSP90) and caveolin-1 (Cav-1) (Brouet et al., 2001a; Brouet et al., 2001b; Fontana et al., 2002). Binding of HSP90 ensures recruitment of activated Akt to the eNOS–HSP90 complex and, thus, phosphorylation of eNOS (Brouet et al., 2001a). These observations suggest that the association of HSP90 and Akt with eNOS is critical in eNOS-associated NO production. Caveolae are flask-shaped vesicular invaginations in the plasma membrane and are considered as a subset of lipid rafts (Anderson, 1998; Smart et al., 1999). They are highly enriched in cholesterol, sphingomyelin, glycolipids, caveolins, signal transducing molecules such as eNOS and phosphatidylinositol 3-kinase (PI3K) and lipoprotein receptors such as SR-BP and CD36 (Babitt et al., 1997; Brown and Rose, 1992; Lisanti et al., 1994; Liu and Anderson, 1995; Shaul et al., 1996; Smart et al., 1994). Cav-1, a caveolae-coat associate protein, is known to important in trafficking cholesterol between endoplamic reticulum and plasma membrane (Smart et al., 1996). Cav-1 is also

a negative regulator of eNOS enzymatic activity by reversibly keeping the enzyme in an inactive state (Garcia-Cardena et al., 1997). Agonists that increase intracellular Ca^{2+} concentration, such as bradykinin, promote Cav-1 dissociation from eNOS. This results in eNOS activation and translocation to sites within the cytosol. The cycle may be reversed by a return of intracellular Ca^{2+} levels to baseline(Meye et al., 2007). eNOS activity is regulated by Ca^{2+}-calmodulin, phosphorylation, and interactions with caveolin-1 (Maniatis et al., 2006; Sessa, 2004). Activation of kinases such as Akt can lead to eNOS activation and its dissociation from Cav-1 (Williams and Lisanti, 2004). Thus the regulation of eNOS by substrate and cofactor dependence, phosphorylation, and interaction with caveolin might all affect the level of bioavailable NO.

Garlic (*Allium sativum* L.) has been used as a flavoring and medicinal agent for hundreds of years in many countries. It possesses diverse biological activities, including antitumorigenesis, antidiabetes, antioxidation, hepatic protection, and immune modulation effects (Agarwal, 1996; Rivlin, 2001). Evidence indicates that those health-related functions of garlic can be greatly attributed to its rich content of various organosulfur compounds (OSCs) e.g. allicin, diallyl sulfide, diallyl disulfide, and S-allyl cysteine etc. (Amagase, 2006; Neil and Silagy, 1994). Regarding to eNOS activity, garlic extract is effective on activation of eNOS activity which leads to the suppression of aggregation in isolated platelet (Berliner and Heinecke, 1996). In addition, in human umbilical vein endothelial cells (HUVEC) in vitro, garlic aqueous extract and S-allyl cysteine (SAC) have been demonstrated to increase NO bioavailability, as judged by measuring cGMP production (Kim et al., 2001; Maslin et al., 1997; Sooranna et al., 1995). However, there is no experimental evidence available to show the exact mechanism of endothelium NOS activation mediated by garlic.

In endothelial cells, Akt activation has been reported to promote cell survival and activate eNOS, which leads to nitric oxide (NO) production (Fulton et al., 1999). It has also been reported that the PI3K/Akt/NO pathway plays an important role in preventing oxLDL-induced endothelial cell injury (Chavakis et al., 2001). In the present study, we hypothesized that the potent protection of garlic against oxLDL suppression of eNOS activation is likely to act on maintaing normal eNOS localization and function. To test this hypothesis, the effect of two garlic organosulfur compounds, diallyl disulfide (DADS) and diallyl trisulfide (DATS), on eNOS and Akt activation and also the association of eNOS and caveolin-1 in oxLDL-treated HUVEC were examined.

Materials and Methods

Materials

HUVECs were obtained from Clonetics Co. (San Diego, CA). DAS and DADS were purchased from Fluka Chemical Co. (Buchs, Switzerland). DATS was purchased from LKT Laboratories (St. Paul, MN). Medium 199 was from Gibco-BRL (Grand Island, NY). Monoclonal antibody to Hsp90 was purchased from StressGen Biotechnologies Co. (British Columbia, Canada). Polyclonal antibodies to PKB, phospho-PKB (Ser473), eNOS, and phospho-eNOS (Ser1177) were obtained from Cell Signaling Technology (Beverly, MA) and Upstate Cell Signaling Solutions (New

York, NY). Polyclonal antibodies to caveolin-1 and Compartmental protein extraction kit were purchased from Chemicon International (Temecula, CA). HEPES, heparin, $CuSO_4$, 4,5-diaminofluorescein diacetate (DAF-2 DA), actinomycin D, cycloheximide, wortmannin, H89, and actin antibody were obtained from Sigma (St. Louis, MO). Z-Leu-Leu-Leu-CHO (MG132) was purchased from Boston Biochem (Cambridge, MA). cGMP assay kit was from Cayman Chemical (Ann Arbor, MI). PP2 was purchased from Biomol (Plymouth Meeting, PA).

Cell cultures

HUVEC with passages between 7 and 9 were used in this study. Cells were grown in 10 mL of medium 199 supplemented with 20 mmol/L HEPES (pH 7.4), 30 mg/L endothelial cell growth supplement (Upstate Biotechnology, Lake Placid, NY), 100 mg/L heparin, 20% fetal bovine serum (FBS, Biological Industries, Canada), 100,000 U/L penicillin, and 100 mg/L streptomycin at 37°C under 5% CO_2.

LDL isolation and ox-LDL preparation

Blood was collected from healthy volunteers to isolate LDL. Written informed consent as approved by the Review Board for Human Research of the Chung-Shan Medical University was signed by all participants. Plasma in the presence of EDTA was used to isolate LDL by sequential ultracentrifugation ($1.019 < d < 1.063$ kg/L) (Claise et al., 1999). Afterward, native LDL was dialyzed at 4°C for 48 h against 500 volumes of phosphate buffered saline (PBS) to remove EDTA. To initiate oxidation, LDL in an amount of 0.5 g/L protein was exposed to 5 μmol/L $CuSO_4$ for 18 h. The generation of thiobarbituric acid-reactive substances was monitored by the fluorometric method as described by Fraga et al. (Fraga et al., 1988), and the values of malondialdehyde equivalents increased from 0.76 ± 0.21 nmol/mg protein of native LDL to 17.8 ± 1.6 nmol/mg protein of $CuSO_4$–treated LDL. The freshly prepared ox-LDL was dialyzed at 4°C for 48 h against 500 volumes of PBS to remove Cu^{2+} and was sterilized by passage through a 0.45-μm filter. The protein contents of native LDL and the ox-LDL preparations were measured by the Lowry assay (Lowry et al., 1951).

Cell treatments

For each experiment, HUVEC at 80% confluence were incubated with DADS or DATS at the indicated concentrations for 16 h and then stimulated with 40 mg/L of ox-LDL for an additional 24 h. Cells were lysed in a phosphorylation lysis buffer (50 mmol/L HEPES, 150 mmol/L NaCl, 200 μmol/L sodium orthovanadate, 10 mmol/L sodium pyrophosphate, 1 mmol/L sodium fluoride, 1 mmol/L EDTA, 1.5 mmol/L magnesium chloride, 10% glycerol, 1% Triton X-100, 1 mmol/L PMSF, and 10 mg/L aprotinin). The cell lysates were then sonicated at 20 W for 15 s in ice bath. All of the cell extracts were centrifuged at 20,000 ×g at 4°C for 15 min. The supernatants were recovered and the total protein was analyzed by the Commassie Plus protein assay reagent kit (Pierce Biotechnology Inc., Rockford, IL).

Immunoprecipitation and Western blot analysis

The membrane and cytoplasmic fractions were prepared by Compartmental protein extraction kit. The membrane protein (600 μg) was incubated with 5 μg of anti caveolin-1 antibody for overnight with rotation at 4°C. 20 μl protein-A sepharose was added for 2 h with rotation at 4°C. Immunoprecipitates were collected by centrifugation, washed three times with IP buffer plus 0.5% deoxycholate, five times with IP buffer alone, and subjected to SDS–PAGE. Equal amounts of total cellular proteins were then electrophoresed in a SDS-polyacrylamide gel, and proteins were then transferred to PVDF membranes (Amersham Biosciences Co., Piscataway, NJ). Nonspecific binding sites on the membranes were blocked with 5% nonfat milk at 4°C overnight. Membranes were probed with rabbit anti-PKB, phospho-PKB, eNOS, phospho-eNOS, and β-actin antibody or mouse anti-Hsp90. The membranes were then probed with their respective secondary antibody labeled with horseradish peroxidase. The bands were visualized by using an enhanced chemiluminescence kit (Perkin Elmer Life Science, Boston, MA) and quantitated with an AlphaImager 2000 (Alpha Innotech).

RT-PCR for eNOS and caveolin-1

Total RNA of HUVEC was extracted by using Trizol reagent (Life Technologies Inc., Rockville, MD). Four micrograms of total RNA was used for the synthesis of first-strand cDNA by using M-MLV Reverse Transcriptase (Promega, Madison, WI) in a 20-μl final volume containing 250 ng oligo-dT and 40 units RNase inhibitor. PCR was carried out in a thermocycler in a 50-μl reaction volume containing 20 μl of cDNA, BioTaq PCR buffer, 50 μM of each dNTP, 1.25 mmol/L $MgCl_2$, and 1 unit of BioTaq DNA polymerase (BioLine, Randolph, MA). Oligonucleotide primers of eNOS (forward: 5'-CAAGGGCACCGGCATCACCA-3', reverse: 5'-CGCCGCCAAGAGGACA -CCAGT-3'), caveolin-1 (forward: 5'-CCTCCTCACAGTTTTCATCC-3', reverse: 5'-CAATCACAT -CTTCAAAGTCAATC-3'), and GAPDH (forward: GAGTCAACGGATTTGGTCGT, reverse: TTGATTTTGGAGGGATC TCG) were designed on the basis of published sequences (Meye et al., 2007). Amplification was performed under standard conditions: denaturation at 94°C for 1 min, 32 cycles of amplification with annealing at 50°C for 1 minute, and extension at 72°C for 1 minute. The GAPDH cDNA level was used as the internal standard. PCR products were resolved in a 1%-agarose gel and were scanned by using a Digital Image Analyzer (Alpha Innotech, San Leandro, CA) and quantitated with an AlphaImager 2000 (Alpha Innotech).

Measurement of intracellular cGMP concentrations

HUVEC were pretreated with each of garlic allyl sulfides and then exposed to ox-LDL for an additional 24 h as stated above. At the end of treatment, HUVEC were placed on an ice bath and incubated for 60 min with 0.1 N HCl. Intracellular cGMP concentrations were measured by using the cGMP EIA kit obtained from Cayman Chemical.

Results

eNOS phosphorylation and interaction with Cav-1

To determine whether garlic allyl sulfides protect eNOS activation against oxLDL insult, an immunoblot assay was performed. With oxLDL alone, the levels of both total eNOS and phosphorylated eNOS were decreased as compared to the control cells (**Fig. 1A**). In the presence of DADS and DATS pretreatment, a dose-dependent restoration of decrease of total eNOS and eNOS phosphorylation was noted, suggesting two allyl sulfides act not only on protein preservation but also on enzyme activation. In contrast, DAS even at a concentration of 1000 μM showed minor protection. eNOS activation is known to be associated with its interaction with Cav-1, and oxLDL decreases the association of eNOS with membrane Cav-1. Therefore, an immunoprecipitation assay was performed to examine whether Cav-1/eNOS colocalization is affected by DADS and DATS. As indicated in **Fig 1B**, decrease of Cav-1-associated eNOS by oxLDL was reversed by DADS and DATS but no by DAS.

PKB and eNOS activation

Src-PI3-K/PKB signaling pathway is known to involve in eNOS phosphorylation on Ser 1177. In the presence of DADS and DATS, oxLDL suppression of PKB phosphorylation was dose-dependently reversed (**Fig. 2A**). As compared to oxLDL alone, a 54.2% and 88.7% increase of phosphorylated PKB was detected in 100 μM DADS and 20 μM DATS treated cells, respectively. Again, DAS had no protection on PKB phosphorylation. Based on these results, DADS and DATS with a concentration of 200 μM and 50 μM, respectively, were tested in the following experiments.

Next, the protection of garlic allyl sulfides was examined in the presence of PI3K, and Src inhibitors. As noted, DADS and DATS effectively reversed the decrease of total eNOS and phosphorylated eNOS contents resulted by oxLDL (**Fig. 2B**). With PKB inhibitor wortmannin, and Src-kinase inhibitor PP2 pretreatment, the recovery in eNOS phosporylation by DADS and DATS disappeared, suggesting Src-PI3K signaling pathway plays a role in the garlic allyl sulfides maintenance of eNOS activation in the presence of oxLDL.

DADS and DATS on eNOS mRNA stability and protein degradation

In addition to working through eNOS activation, it is interesting to note that DADS and DATS effectively reverse the reduction of total eNOS level resulted by oxLDL. This raises a possibility whether garlic allyl sulfides act on the stage of eNOS transcription and also on protein turnover. First, a RT-PCR was performed to determine eNOS mRNA level in the presence of transcription inhibitor, actinomycin D. As noted, regardless the presence or absence of actinomycin D, oxLDL and allyl sulfides caused no changes in mRNA level (**Fig. 3**).

DADS and DATS influenced cGMP levels in HUVECs

We finally determined the cellular changes of cGMP production by garlic allyl sulfides in the presence of ox-LDL. As noted for the inhibition of NO production, ox-LDL caused HUVEC a marked decrease of cGMP level by 33.5% ($P<0.05$) (**Fig. 4**). With 200 μmol/L DADS or 20 μmol/L

DATS pretreatment, cGMP content returned to normal concentration as noted in control cells. Again, wortmannin blocked DADS and DATS protection on cGMP production in HUVEC.

Conclusion

In the present study, we demonstrated that the potent protection of garlic against oxLDL suppression of eNOS activation is likely to act on maintaing normal eNOS localization and function. In addition, the effect of two garlic organosulfur compounds, diallyl disulfide (DADS) and diallyl trisulfide (DATS), on eNOS and Akt activation and also the association of eNOS and caveolin-1 in oxLDL-treated HUVEC. Furthermore, DADS and DATS have been also demonstrated to increase NO bioavailability, as judged by measuring cGMP production

Reference

Agarwal, K. C. (1996). Therapeutic actions of garlic constituents. Med Res Rev *16*, 111-124.

Alderton, W. K., Cooper, C. E., and Knowles, R. G. (2001). Nitric oxide synthases: structure, function and inhibition. Biochem J *357*, 593-615.

Amagase, H. (2006). Clarifying the real bioactive constituents of garlic. J Nutr *136*, 716S-725S.

Anderson, R. G. (1998). The caveolae membrane system. Annu Rev Biochem *67*, 199-225.

Babaev, V. R., Patel, M. B., Semenkovich, C. F., Fazio, S., and Linton, M. F. (2000). Macrophage lipoprotein lipase promotes foam cell formation and atherosclerosis in low density lipoprotein receptor-deficient mice. J Biol Chem *275*, 26293-26299.

Babitt, J., Trigatti, B., Rigotti, A., Smart, E. J., Anderson, R. G., Xu, S., and Krieger, M. (1997). Murine SR-BI, a high density lipoprotein receptor that mediates selective lipid uptake, is N-glycosylated and fatty acylated and colocalizes with plasma membrane caveolae. J Biol Chem *272*, 13242-13249.

Berliner, J. A., and Heinecke, J. W. (1996). The role of oxidized lipoproteins in atherogenesis. Free Radic Biol Med *20*, 707-727.

Blair, A., Shaul, P. W., Yuhanna, I. S., Conrad, P. A., and Smart, E. J. (1999). Oxidized low density lipoprotein displaces endothelial nitric-oxide synthase (eNOS) from plasmalemmal caveolae and impairs eNOS activation. J Biol Chem *274*, 32512-32519.

Bredt, D. S. (1999). Endogenous nitric oxide synthesis: biological functions and pathophysiology. Free Radic Res *31*, 577-596.

Brouet, A., Sonveaux, P., Dessy, C., Balligand, J. L., and Feron, O. (2001a). Hsp90 ensures the transition from the early Ca2+-dependent to the late phosphorylation-dependent activation of the endothelial nitric-oxide synthase in vascular endothelial growth factor-exposed endothelial cells. J Biol Chem *276*, 32663-32669.

Brouet, A., Sonveaux, P., Dessy, C., Moniotte, S., Balligand, J. L., and Feron, O. (2001b). Hsp90 and caveolin are key targets for the proangiogenic nitric oxide-mediated effects of statins. Circ Res *89*, 866-873.

Brown, D. A., and Rose, J. K. (1992). Sorting of GPI-anchored proteins to glycolipid-enriched membrane subdomains during transport to the apical cell surface. Cell *68*, 533-544.

Chavakis, E., Dernbach, E., Hermann, C., Mondorf, U. F., Zeiher, A. M., and Dimmeler, S. (2001). Oxidized LDL inhibits vascular endothelial growth factor-induced endothelial cell migration by an inhibitory effect on the Akt/endothelial nitric oxide synthase pathway. Circulation *103*, 2102-2107.

Claise, C., Edeas, M., Chaouchi, N., Chalas, J., Capel, L., Kalimouttou, S., Vazquez, A., and Lindenbaum, A. (1999). Oxidized-LDL induce apoptosis in HUVEC but not in the endothelial cell line EA.hy 926. Atherosclerosis *147*, 95-104.

Feron, O., Michel, J. B., Sase, K., and Michel, T. (1998). Dynamic regulation of endothelial nitric oxide synthase: complementary roles of dual acylation and caveolin interactions. Biochemistry *37*, 193-200.

Fontana, J., Fulton, D., Chen, Y., Fairchild, T. A., McCabe, T. J., Fujita, N., Tsuruo, T., and Sessa, W. C. (2002). Domain mapping studies reveal that the M domain of hsp90 serves as a molecular scaffold to regulate Akt-dependent phosphorylation of endothelial nitric oxide synthase and NO

release. Circ Res *90*, 866-873.

Fulton, D., Gratton, J. P., McCabe, T. J., Fontana, J., Fujio, Y., Walsh, K., Franke, T. F., Papapetropoulos, A., and Sessa, W. C. (1999). Regulation of endothelium-derived nitric oxide production by the protein kinase Akt. Nature *399*, 597-601.

Fraga, C.G., Leibovitz, B.E., and Tappel, A.L. (1988). Lipid peroxidation measured as thiobarbituric acid-reactive substances in tissue slices: characterization and comparison with homogenates and microsomes. Free Radic Biol Med *4*, 155-161.

Garcia-Cardena, G., Fan, R., Shah, V., Sorrentino, R., Cirino, G., Papapetropoulos, A., and Sessa, W. C. (1998). Dynamic activation of endothelial nitric oxide synthase by Hsp90. Nature *392*, 821-824.

Garcia-Cardena, G., Martasek, P., Masters, B. S., Skidd, P. M., Couet, J., Li, S., Lisanti, M. P., and Sessa, W. C. (1997). Dissecting the interaction between nitric oxide synthase (NOS) and caveolin. Functional significance of the nos caveolin binding domain in vivo. J Biol Chem *272*, 25437-25440.

Ji, Y., Diao, J., Han, Y., Huang, Y., Bai, H., Chen, Q., Fan, L., and Ferro, A. (2006). Pyridoxine prevents dysfunction of endothelial cell nitric oxide production in response to low-density lipoprotein. Atherosclerosis *188*, 84-94.

Kawashima, S. (2004). Malfunction of vascular control in lifestyle-related diseases: endothelial nitric oxide (NO) synthase/NO system in atherosclerosis. J Pharmacol Sci *96*, 411-419.

Kim, K. M., Chun, S. B., Koo, M. S., Choi, W. J., Kim, T. W., Kwon, Y. G., Chung, H. T., Billiar, T. R., and Kim, Y. M. (2001). Differential regulation of NO availability from macrophages and endothelial cells by the garlic component S-allyl cysteine. Free Radic Biol Med *30*, 747-756.

Lisanti, M. P., Scherer, P. E., Vidugiriene, J., Tang, Z., Hermanowski-Vosatka, A., Tu, Y. H., Cook, R. F., and Sargiacomo, M. (1994). Characterization of caveolin-rich membrane domains isolated from an endothelial-rich source: implications for human disease. J Cell Biol *126*, 111-126.

Liu, J., Garcia-Cardena, G., and Sessa, W. C. (1995). Biosynthesis and palmitoylation of endothelial nitric oxide synthase: mutagenesis of palmitoylation sites, cysteines-15 and/or -26, argues against depalmitoylation-induced translocation of the enzyme. Biochemistry *34*, 12333-12340.

Liu, P., and Anderson, R. G. (1995). Compartmentalized production of ceramide at the cell surface. J Biol Chem *270*, 27179-27185.

Lloyd-Jones, D. M., and Bloch, K. D. (1996). The vascular biology of nitric oxide and its role in atherogenesis. Annu Rev Med *47*, 365-375.

Loscalzo, J., and Welch, G. (1995). Nitric oxide and its role in the cardiovascular system. Prog Cardiovasc Dis *38*, 87-104.

Lowry, O.H., Rosebrough, N.J., Farr, A.L., and Randall, R.J. (1951). Protein measurement with the Folin phenol reagent. J Biol Chem *193*, 265-275.

Maniatis, N. A., Brovkovych, V., Allen, S. E., John, T. A., Shajahan, A. N., Tiruppathi, C., Vogel, S. M., Skidgel, R. A., Malik, A. B., and Minshall, R. D. (2006). Novel mechanism of endothelial nitric oxide synthase activation mediated by caveolae internalization in endothelial cells. Circ Res *99*, 870-877.

Maslin, D. J., Brown, C. A., Das, I., and Zhang, X. H. (1997). Nitric oxide--a mediator of the effects of garlic? Biochem Soc Trans *25*, 408S.

Meye, C., Schumann, J., Wagner, A., and Gross, P. (2007). Effects of homocysteine on the levels of

caveolin-1 and eNOS in caveolae of human coronary artery endothelial cells. Atherosclerosis *190*, 256-263.

Michel, J. B., Feron, O., Sacks, D., and Michel, T. (1997). Reciprocal regulation of endothelial nitric-oxide synthase by Ca2+-calmodulin and caveolin. J Biol Chem *272*, 15583-15586.

Moncada, S., and Higgs, E. A. (2006). The discovery of nitric oxide and its role in vascular biology. Br J Pharmacol *147 Suppl 1*, S193-201.

Morawietz, H., Duerrschmidt, N., Niemann, B., Galle, J., Sawamura, T., and Holtz, J. (2001). Induction of the oxLDL receptor LOX-1 by endothelin-1 in human endothelial cells. Biochem Biophys Res Commun *284*, 961-965.

Neil, A., and Silagy, C. (1994). Garlic: its cardio-protective properties. Curr Opin Lipidol *5*, 6-10.

Rivlin, R. S. (2001). Historical perspective on the use of garlic. J Nutr *131*, 951S-954S.

Ross, R. (1993). The pathogenesis of atherosclerosis: a perspective for the 1990s. Nature *362*, 801-809.

Sessa, W. C. (2004). eNOS at a glance. J Cell Sci *117*, 2427-2429.

Shaul, P. W., Smart, E. J., Robinson, L. J., German, Z., Yuhanna, I. S., Ying, Y., Anderson, R. G., and Michel, T. (1996). Acylation targets emdothelial nitric-oxide synthase to plasmalemmal caveolae. J Biol Chem *271*, 6518-6522.

Smart, E. J., Graf, G. A., McNiven, M. A., Sessa, W. C., Engelman, J. A., Scherer, P. E., Okamoto, T., and Lisanti, M. P. (1999). Caveolins, liquid-ordered domains, and signal transduction. Mol Cell Biol *19*, 7289-7304.

Smart, E. J., Ying, Y., Donzell, W. C., and Anderson, R. G. (1996). A role for caveolin in transport of cholesterol from endoplasmic reticulum to plasma membrane. J Biol Chem *271*, 29427-29435.

Smart, E. J., Ying, Y. S., Conrad, P. A., and Anderson, R. G. (1994). Caveolin moves from caveolae to the Golgi apparatus in response to cholesterol oxidation. J Cell Biol *127*, 1185-1197.

Sooranna, S. R., Hirani, J., and Das, I. (1995). Garlic can induce both GTP cyclohydrolase and nitric oxide synthase activity in choriocarcinoma cells. Biochem Soc Trans *23*, 543S.

Steinberg, D. (1997). Low density lipoprotein oxidation and its pathobiological significance. J Biol Chem *272*, 20963-20966.

Williams, T. M., and Lisanti, M. P. (2004). The Caveolin genes: from cell biology to medicine. Ann Med *36*, 584-595.

Witztum, J. L., and Steinberg, D. (1991). Role of oxidized low density lipoprotein in atherogenesis. J Clin Invest *88*, 1785-1792.

Xu, H. S., Duan, J., Dai, S., Wu, Y., Sun, R., and Ren, J. (2004). Phytoestrogen alpha-zearalanol antagonizes oxidized LDL-induced inhibition of nitric oxide production and stimulation of endothelin-1 release in human umbilical vein endothelial cells. Endocrine *25*, 235-245.

Zmijewski, J. W., Moellering, D. R., Le Goffe, C., Landar, A., Ramachandran, A., and Darley-Usmar, V. M. (2005). Oxidized LDL induces mitochondrially associated reactive oxygen/nitrogen species formation in endothelial cells. Am J Physiol Heart Circ Physiol *289*, H852-861.

Fig. 1.

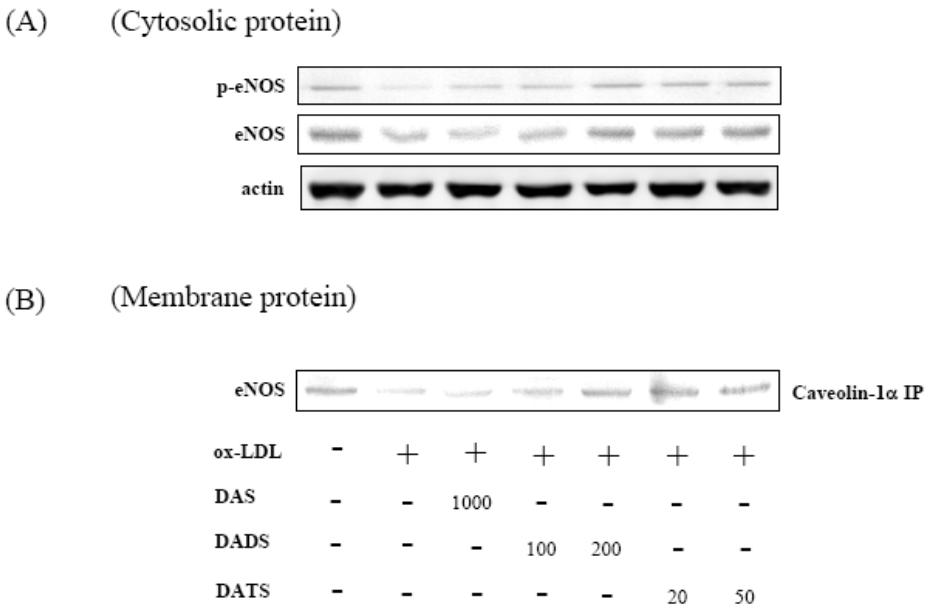

FIGURE 1 DADS and DATS increase eNOS-Cav-1 interaction and phosphorylation in HUVECs. Cells were treated with DAS (1 mmol/L), DADS (100-200 μmol/L) or DATS (20-50 μmol/L) for 16 h and were then incubated with 40 mg/L ox-LDL for an additional 24 h. The cytopalsmic protein was analyzed by western blotting for the presence of eNOS and the phosphorylation of eNOS (A). eNOS-Cav-1 interaction in cellular membrane was examined by immunoprecipitation (IP) with an antibody to Cav-1 followed by immunoblotting with eNOS antibody (B).

Fig. 2

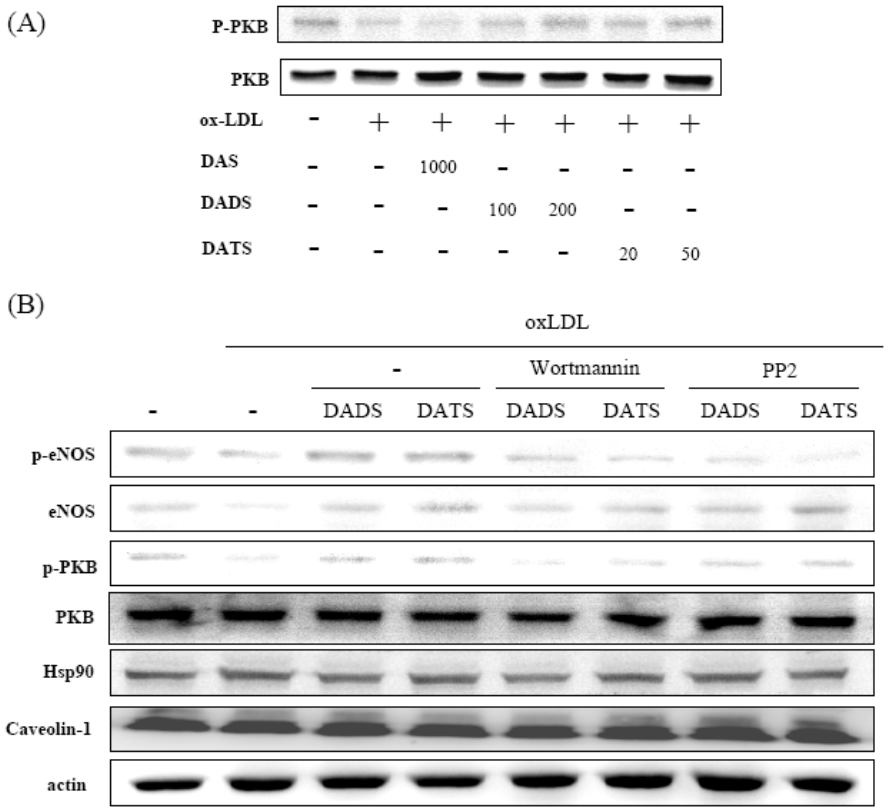

FIGURE 2 Effects of protein kinase inhibitors on DADS or DATS change in oxLDL-inhibited phosphorylation of eNOS. Cells were incubated with either 200 mmol/L DADS or 20 mmol/L DATS for 16 h and were then treated with 40 mg/L ox-LDL for an additional 24 h. The cytopalsmic protein was analyzed by western blotting for the presence of PKB and the phosphorylation of PKB (A). For inhibitor treatments, wortmannin (100 nmol/L) or PP2 (10 μmol/L) was added 1 h before the addition of DADS or DATS (B).

Fig. 3

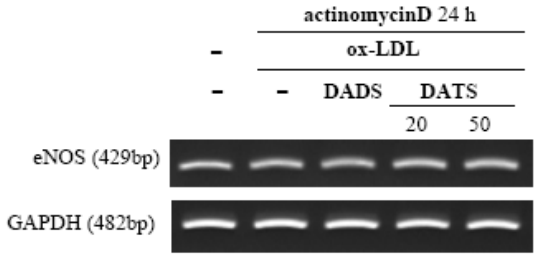

FIGURE 3 Effect of DADS and DATS on the stability of eNOS mRNA inhibited by ox-LDL. The cells were pretreated with 200 mmol/L DADS or 20 mmol/L DATS in the presence of actinomycin D (1 μg/ml) for 16 h followed by stimulation with 40 mg/L ox-LDL. Analysis of mRNA expression of eNOS, Cav-1, and GAPDH was performed by RT-PCR.

Fig. 4

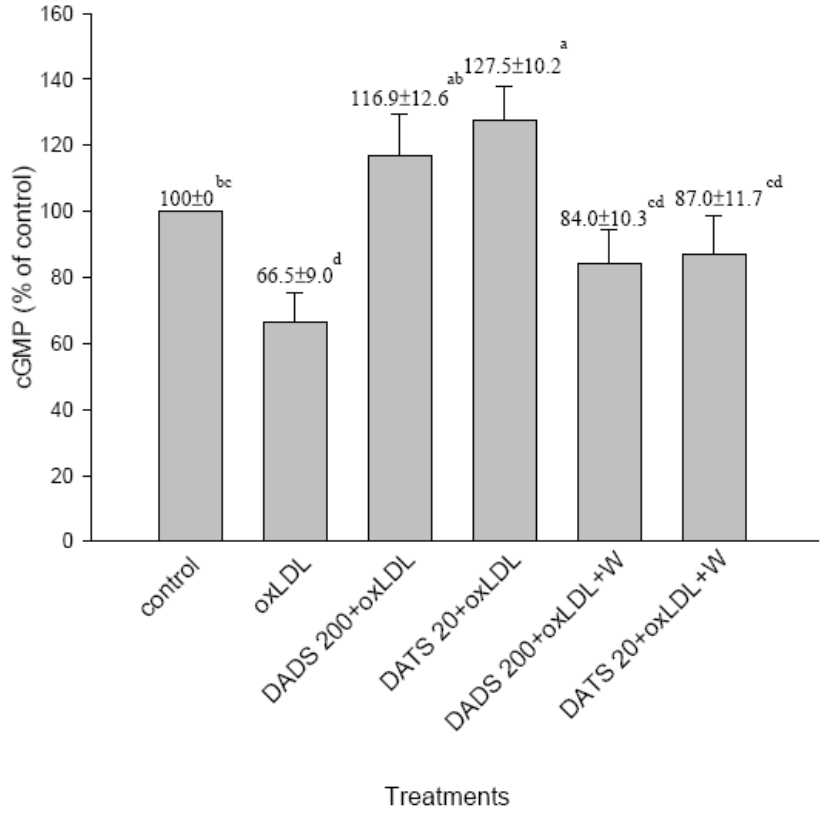

FIGURE 4 Measurement of cGMP production in HUVECs during incubation with DADS and DATS in presence or absence of inhibitors of PKA and PKB. HUVECs were preincubated with 200 μmol/L DADS or 100 μmol/L DATS for 16 h and were then stimulated by 40 mg/L ox-LDL for an additional 24 h. Wortmannin (100 nmol/L) or H89 (5 μmol/L) was added 1 h before allyl sulfide treatment. Values represent mean ± SD (n = 3); Groups not sharing a common letter differ significantly, $P < 0.05$.